

腮腺 CT 影像报告与数据系统的初步研究

李玉冰^{1*} 孙丽莎^{2*} 孙志鹏^{1△} 谢晓艳¹ 张建运³ 张祖燕¹ 赵燕平¹ 马绪臣¹

(北京大学口腔医学院·口腔医院, 1. 医学影像科; 2. 中心实验室; 3. 口腔病理科 国家口腔疾病临床医学研究中心 口腔数字化医疗技术和材料国家工程实验室 口腔数字医学北京市重点实验室, 北京 100081)

[摘要] 目的: 初步建立腮腺 CT 影像报告与数据系统(Parotid Imaging Reporting and Data System, PI-RADS), 并探讨其临床应用价值。方法: 纳入 2013 年 1 月至 2016 年 12 月间因腮腺肿物就诊于北京大学口腔医院并进行手术治疗的病例, 回顾性评估所有病例的影像资料, 获取相关影像特征, 评估肿瘤恶性风险概率, 并分为 6 个等级(1 级, 正常腮腺; 2 级, 基本确定为良性病变或肿瘤; 3 级, 无明确恶性病变证据但不能确定为良性病变; 4 级, 怀疑为恶性肿瘤病变但证据不充分; 5 级, 恶性肿瘤影像征象较充分; 6 级, 有恶性肿瘤病理学证据)。结果: 共纳入腮腺肿物病例 897 例次, 其中良性病变 905 例次、恶性肿瘤 98 例次, 影像诊断为 2 级、3 级、4 级和 5 级的病变中, 恶性肿瘤的构成比分别为 0.4%、5.7%、35.5% 和 96.7%。随 PI-RADS 分级呈逐渐增高趋势($Z = -15.579, P < 0.001$)。相邻等级[2 级与 3 级($\chi^2 = 12.048, P = 0.001$)、3 级与 4 级($\chi^2 = 75.231, P < 0.001$)、4 级与 5 级($\chi^2 = 32.266, P < 0.001$)]之间的恶性构成比差异有统计学意义。Cohen's Kappa 检验表明两位研究者分级诊断具有中度一致性($\kappa = 0.614, P < 0.001, 95\% CI: 0.569 \sim 0.695$)。结论: 应用影像诊断分级方法对腮腺肿瘤性疾病的诊断和临床治疗有一定的帮助。

[关键词] 腮腺肿瘤; 体层摄影术, X 线计算机; 诊断, 鉴别; 治疗

[中图分类号] R739.87 [文献标志码] A [文章编号] 1671-167X(2020)01-0083-07

doi: 10.19723/j.issn.1671-167X.2020.01.013

Parotid CT imaging reporting and data system: A preliminary study

LI Yu-bing^{1*}, SUN Li-sha^{2*}, SUN Zhi-peng^{1△}, XIE Xiao-yan¹, ZHANG Jian-yun³, ZHANG Zu-yan¹, ZHAO Yan-ping¹, MA Xu-chen¹

(1. Department of Oral and Maxillofacial Radiology, 2. Central Laboratory, 3. Department of Oral Pathology, Peking University School and Hospital of Stomatology & National Clinical Research Center for Oral Diseases & National Engineering Laboratory for Digital and Material Technology of Stomatology & Beijing Key Laboratory of Digital Stomatology, Beijing 100081, China)

ABSTRACT Objective: To establish a Parotid Imaging Reporting and Data System (PI-RADS) for CT diagnosis of the parotid gland neoplasms and to investigate the clinical applicable value and feasibility of PI-RADS. **Methods:** Patients who had been diagnosed with primary parotid gland neoplasms and had received surgical treatments in Peking University School and Hospital of Stomatology during the period of January 2013 to December 2016 were included in this study. The diagnoses were confirmed by the post-operative pathological examinations in all the patients. The CT imaging data of all patients were retrospectively reviewed and analyzed by two readers in consensus. Imaging characteristics related to the parotid neoplasms were extracted and quantified. Based on comprehensive analysis of the imaging characteristics, the probabilities of the benign and malignant neoplasms were evaluated and classified into six grades, PI-RADS 1-6 (PI-RADS 1: normal parotid gland; PI-RADS 2: confidently benign lesions; PI-RADS 3: probably benign lesions without confirmed evidence of malignancy; PI-RADS 4: suspected malignancy without sufficient evidence of malignancy; PI-RADS 5: confidently malignant lesions; PI-RADS 6: lesions with confirmed pathological evidence of malignancy). **Results:** A total of 897 patients with 1 003 parotid lesions were included. The lesions included 905 benign and 98 malignant lesions. The proportions of the malignancies in PI-RADS 2, PI-RADS 3, PI-RADS 4 and PI-RADS 5 according to the two readers in consensus were 0.4%, 5.7%, 35.5% and 96.7% respectively. The overall Cohen's Kappa test showed medium consistency between the two independent researchers ($\kappa = 0.614, P < 0.001, 95\% CI: 0.569 \sim 0.695$). Pearson Chi-square test showed that the proportions of malignancies increased with the diagnostic PI-RADS grades (Cochran-Armitage trend test, $Z = -15.579, P < 0.001$). The results of Pearson Chi-square tests showed significant differences between the grades [PI-RADS 2 and 3 ($\chi^2 = 12.048, P = 0.001$); PI-RADS 3 and 4 ($\chi^2 = 75.231, P < 0.001$); PI-RADS 4 and 5 ($\chi^2 = 32.266,$

△ Corresponding author's e-mail, sunzhipeng@bjmu.edu.cn

* These authors contributed equally to this work

网络出版时间: 2019-12-27 15:22:31 网络出版地址: <http://kns.cnki.net/kcms/detail/11.4691.R.20191227.1309.006.html>

$P < 0.001$]。 **Conclusion:** PI-RADS can be used to evaluate the risk of malignancy and will be helpful to improve the imaging diagnosis and clinical treatment of parotid gland neoplasms.

KEY WORDS Parotid neoplasms; Tomography , X-ray computed; Diagnosis , differential; Therapy

唾液腺肿瘤是常见的口腔疾病^[1] ,约占全身肿瘤的3%^[2] ,其中80%发生于腮腺^[3]。腮腺肿瘤病理学种类繁多^[4] ,多形性腺瘤和 Warthin 瘤等良性肿瘤占80%左右。恶性腮腺肿瘤的临床表现有较大差异^[5] ,部分恶性肿瘤的临床和影像表现缺少特异性 ,在术前难以准确判断其性质^[6]。

超声、CT 和磁共振成像等为常用的腮腺肿瘤影像学检查方法^[7]。CT 通过分析腮腺肿瘤的大小、部位、边界和强化特征等能够初步判断其性质^[7] ,对于 Warthin 瘤等部分肿瘤可以较准确地诊断 ,但对于多形性腺瘤和部分恶性肿瘤的鉴别则存在一定的困难。因此 ,传统影像诊断方法较难实现规范化诊断报告。

甲状腺肿瘤等疾病的临床实践证明 ,应用影像报告与数据系统对肿瘤的恶性概率作出等级评估有利于肿瘤的诊疗^[8-9] ,能够提高肿瘤影像学诊断对临床的指导意义。腮腺肿瘤的临床实践中尚未见应用影像报告与数据系统 ,因此 ,本研究拟初步建立一个基于 CT 的腮腺影像报告与数据系统 (Parotid Imaging Reporting and Data System ,PI-RADS) ,探讨和研究腮腺肿瘤恶性概率等级评估方法 ,以进一步提高腮腺肿瘤临床诊疗的规范化水平和科研水平。

1 资料与方法

1.1 研究对象

纳入 2013 年 1 月至 2016 年 12 月间因原发性腮腺肿物就诊于北京大学口腔医院的病例 ,所有患者术前均行 CT 检查 and 手术治疗 ,且术后病理诊断明确。排除腮腺复发性肿物、发育异常、涎石症及化脓性炎症疾病。

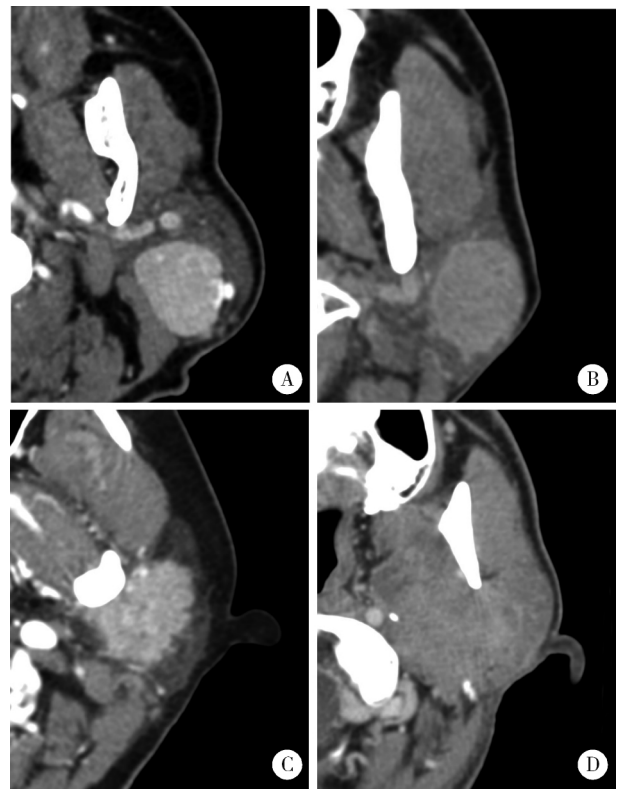
1.2 CT 检查

所有患者于仰卧位进行检查 (GE ,Brightspeed ,Optima CT520 ,USA) 。共 120 例患者 (131 例肿物) 进行 CT 平扫检查 ,411 例患者 (475 例肿物) 进行单期相增强 CT 检查 ,366 例患者 (397 例肿物) 进行多期相增强 CT 检查。单期相或多期相增强 CT 检查于平扫完成后 ,经肘静脉注射对比剂 (碘帕醇 3.7 mg I/mL ,1.5 ~ 2.0 mL/kg 2.0 ~ 3.0 mL/s) ,于注射完成后即刻、30 s 和 5 min 进行增强第一至三相扫描。平扫及增强第一相扫描范围自颅底层至胸锁关节层 ,增强二和三相扫描于病变范围扫描。扫描参数:管电压 120 ~ 140 kV ,管电流 200 ~ 380 mA ,层

厚 1.25 mm ,螺距 1.65 : 1。图像重建参数为:标准重建方式 ,层厚 1.25 mm ,层间距 1.25 mm ,重建视野 20 cm × 20 cm。所有影像资料以 DICOM 格式存储于影像 PACS 系统。

1.3 腮腺肿物影像诊断分级系统

影像分析由两名经验丰富的口腔颌面医学影像专科医师共同商讨决定。于影像诊断系统中评价肿瘤部位、大小、形态、边界、密度、强化特点 (时相、程度、分布) 、肿物单发或多发情况、钙化情况、囊性变情况、周围及颈部淋巴结评估、邻近组织是否被侵犯评估等 (表 1 ,图 1) 。由两名口腔颌面医学影像专科医师独立进行分级诊断 ,并进行一致性评价。



A , a parotid gland neoplasm showing all regular and well-defined oval boundary , characteristic enhancement feature of benign nature (enhancement phase 1) , indicating a PI-RADS 2 tumor. It was proved as Warthin tumor. B , a parotid gland neoplasm showing basically regular and well-defined round boundary , with mild enhancement (enhancement phase 3) , indicating a PI-RADS 3 tumor. It was proved as pleomorphic adenoma. C , a parotid gland neoplasm showing seemingly well-defined boundary , with mild enhancement (enhancement phase 1) , indicating a PI-RADS 4 tumor. It was proved as mucoepidermoid carcinoma. D , a parotid gland neoplasm showing all poorly-defined boundary , with erosion into adjacent structures and mild enhancement (enhancement phase 2) , indicating a PI-RADS 5 tumor. It was proved as adenoid cystic carcinoma.

图 1 PI-RADS 2 级 (A) 、3 级 (B) 、4 级 (C) 、5 级 (D) 诊断的典型病例
Figure 1 A characteristic example of a PI-RADS 2 (A) , 3 (B) , 4 (C) , 5 (D) tumor

表 1 腮腺肿物 PI-RADS 诊断结果与影像学征象

Table 1 Correlations between PI-RADS grades of the parotid gland neoplasms and radiologic signs

Items	PI-RADS 2	PI-RADS 3	PI-RADS 3b	PI-RADS 4	PI-RADS 5	PI-RADS 6	Benign	Malignancy
Size								
Small (<2.0 cm)	30	82	7	7	2	0	118	10
Medium (2.0 - 3.0 cm)	158	453	4	49	14	1	624	55
Large (>3.0 cm)	56	102	1	20	14	3	163	33
Single/multiple								
Single on one side	139	584	0	62	19	3	730	77
Multiple on one side	33	25	5	11	9	1	66	18
Multiple on two sides	72	28	7	3	2	0	109	3
Boundary								
Absolutely clear	153	153	0	3	0	0	309	0
Majorly clear	68	261	2	21	4	0	345	11
Partially ill-defined	17	182	1	26	3	1	210	20
Majorly ill-defined	6	38	7	18	8	3	37	43
Ill-defined	0	3	2	8	15	0	4	24
Shape								
Round	54	269	5	21	7	0	334	22
Oval	154	162	3	13	3	0	322	13
Scalloped	31	182	2	27	6	2	222	28
Irregular	5	24	2	15	14	2	27	35
Dominant density on plain CT								
Fat	7	1	0	0	0	0	8	0
Liquid	30	59	0	4	12	0	91	2
Soft-tissue (partial fluid)	66	239	1	36	18	3	311	46
Soft-tissue	141	338	11	36	0	1	495	50
Enhancement degree on first enhanced phase								
No significant	25	42	0	3	0	0	68	2
Slightly	10	122	0	12	4	0	140	8
Medium	29	203	5	32	13	1	236	47
Obvious	89	114	7	21	11	3	217	28
Significant	67	53	0	5	1	0	119	7
Enhancement pattern								
Gradual	20	294	5	30	11	1	333	28
Fast in-out	124	128	1	23	7	2	254	31
Basically no enhancement	4	4	0	2	1	0	8	3
Gradual in-out	9	51	2	10	2	0	61	13
Enhancement distribution								
Membrane enhancement	5	34	0	7	0	0	40	6
Even	152	182	12	24	15	1	346	36
Uneven to even	17	198	0	21	5	1	223	20
Uneven	14	84	0	17	8	2	99	26
No enhancement	32	36	0	4	0	0	72	0
Calcification								
No	239	602	12	59	26	4	861	81
Small granular or capsule	5	31	0	10	1	0	38	9
Large irregular	0	4	0	7	3	0	6	8
Cystic percentage								
0	177	488	12	49	26	2	683	71
≤25%	19	53	0	10	2	2	72	14
>25% , ≤50%	7	17	0	6	2	0	23	9
>50% , ≤75%	5	33	0	5	0	0	40	3
>75%	36	46	0	6	0	0	87	1
Adjacent structure destruction								
No	237	609	7	64	16	3	867	69
Move	5	19	0	5	0	0	26	3
Poor boundary	2	8	5	6	9	0	12	18
Significant	0	1	0	1	5	1	0	8

PI-RADS , Parotid Imaging Reporting and Data System. The numbers of neoplasms were calculated here.

所有腮腺肿物的影像评价分为 PI-RADS 1 ~ 6 级: PI-RADS 1 级为正常腮腺; PI-RADS 2 级确定为良性病变; PI-RADS 3 级良性病变或肿瘤可能性较大, 无明确恶性肿瘤证据, 但不能排除恶性肿瘤可能

性; PI-RADS 4 级无充分恶性证据但恶性肿瘤可能性增加; PI-RADS 5 级为有确定的恶性肿瘤征象; PI-RADS 6 级为有病理学恶性肿瘤证据。诊断分级具体方法详见表 2。

表 2 腮腺 CT 影像报告与数据系统的诊断标准

Table 2 The diagnostic criteria of PI-RADS

PI-RADS	Criteria
1: Normal parotid gland	There are definitely no masses in the parotid gland
2: More likely benign	(1) Multiple bilateral or unilateral masses presented regular arc border and oval contour with enhancement and without enlarged or necrotic lymph nodes around the parotid gland and neck; (2) A single tumor may also be considered if it is typical (e.g. oval, with obvious and uniform enhancement in the first enhancement phase, with smooth clear border or a low-density fat envelope)
3: Indeterminate	(1) Single, round, no enhancement or uniform enhancement, most of the boundary clear, for example majorly clear or partially ill-defined; (2) Granular with uneven enhancement but definite boundary; (3) Multiple without enhancement, and without enlarged or necrotic lymph nodes around the parotid gland and neck; (4) Small tumors, that means, all tumors diameter less than 1 cm are included, regardless of their enhancement features
3b: Inflammation including Sjögren syndrome and IgG4	In multiple gland, lesions are diffuse, with enhancement, without necrotic lymph nodes around the neck
4: Probably malignant	(1) Single lesion, the shape is slightly irregular, part of the boundary is indistinctly (the boundary marked 3 or 4) or the membrane enhancement with villous edges; (2) The enhancement type is medium enhancement even slightly enhancement, solid lesion with little or without cystic degeneration; (3) Soft tissue density or with partial fluid especially with calcification, a small amount of unilateral diffuse; (4) Have large masses of irregular calcification with swelling lymph nodes but without necrosis lymph nodes
5: Highly suggestive malignancy	(1) Necrotic lymph nodes are seen in the neck; (2) The boundary is unclear, the shape is irregular; (3) The border of the surrounding muscles, bones or fat tissues are not clear, which means destruction
6: Already had malignant diagnosis	Had pathological result to pronounced it is a malignant neoplasm
7: Unsatisfied illustration on CT	The density of neoplasm and the parotid is too nearly to find out what the neoplasm is really like. But couldn't exclude that a neoplasm may exist

PI-RADS, Parotid Imaging Reporting and Data System.

1.4 统计分析

应用 SPSS 20.0 和 SAS 3.7 进行统计分析。计数资料应用卡方检验、Cochran-Armitage 趋势检验等方法进行统计, 计量资料采用单因素方差分析(one way ANOVA), $P < 0.05$ 为差异有统计学意义。计算 kappa 系数评价诊断一致性, kappa 系数 0 ~ 0.20 为较低一致性, 0.21 ~ 0.40 为一般一致性, 0.41 ~ 0.60 为中等一致性, 0.61 ~ 0.80 为高度一致性, 0.81 ~ 1.00 为几乎完全一致。

2 结果

2.1 病例资料

共纳入腮腺肿物患者 897 例, 包括单发肿物 832 例, 多发肿物 64 例; 共 1 003 个肿物, 其中良性肿物 905 个, 恶性肿瘤 98 个。男性 465 例, 女性 432 例, 年龄 4 ~ 85 岁, 平均年龄 46.0 岁。

2.2 PI-RADS 诊断与病理结果

两位研究者共同诊断结果中 PI-RADS 2 级、3 级、3b 级、4 级、5 级和 6 级的构成比分别为 24.3%、

63.5%、1.2%、7.6%、3.0% 和 0.4%。各分级诊断中的病理结果详见表 3。

PI-RADS 2 级、3 级、4 级和 5 级的病变中, 恶性肿瘤构成比分别为 0.4%、5.7%、35.5% 和 96.7%。Cochran-Armitage 趋势检验表明, 随 PI-RADS 诊断分级增高, 恶性肿瘤构成比有增高趋势 ($Z = -15.579, P < 0.001$)。PI-RADS 相邻等级之间恶性肿瘤构成比差异均有统计学意义 [2 级与 3 级 ($\chi^2 = 12.048, P = 0.001$), 3 级与 4 级 ($\chi^2 = 75.231, P < 0.001$), 4 级与 5 级 ($\chi^2 = 32.266, P < 0.001$)]。

多形性腺瘤 (395 例) 诊断为 PI-RADS 2 级、3 级、3b 级、4 级、5 级和 6 级的构成比分别为 1.0%、92.9%、0.5%、0.3%、0。Warthin 瘤 (253 例) 诊断为 PI-RADS 2 级、3 级、3b 级、4 级、5 级和 6 级的构成比分别为 69.6%、28.5%、0.2%、0、0。黏液表皮样癌 (20 例) 诊断为 PI-RADS 2 级、3 级、3b 级、4 级、5 级和 6 级的构成比分别为 5%、30%、0、30%、30%、5%。腺样囊性癌 (7 例) 诊断为 PI-RADS 2 级、3 级、3b 级、4 级、5 级和 6 级的构成比

分别是 0、57.1%、0、0、42.9%、0。腺泡细胞癌 (15 例) 诊断为 PI-RADS 2 级、3 级、3b 级、4 级、5 级和 6 级的构成比分别是 0、86.7%、0、13.3%、0、0。

2.3 PI-RADS 诊断一致性评价

两位读片者的分级诊断判读结果具有中等一致性 $\kappa = 0.614$ (95% 可信区间为 0.569 ~ 0.695), $P < 0.001$ 。

表 3 腮腺肿物病理诊断与 PI-RADS 诊断结果的相关性

Table 3 Correlations between pathological results of the parotid gland neoplasms and PI-RADS grades

Items	PI-RADS 2	PI-RADS 3	PI-RADS 3b	PI-RADS 4	PI-RADS 5	PI-RADS 6	PI-RADS total
Warthin tumor	176	72	0	5	0	0	253
Pleomorphic adenoma	4	367	0	23	1	0	395
Basal cell adenoma	11	81	0	2	0	0	94
Myoepithelioma	0	3	0	0	0	0	3
Oncocytoma	4	4	0	0	0	0	8
Cystadenoma	0	6	0	0	0	0	6
Keratocystoma	0	0	0	1	0	0	1
Cyst	28	14	0	0	0	0	42
Lipoma	4	1	0	0	0	0	5
Schwannoma	0	9	0	0	0	0	9
Vascular malformation	2	9	0	2	0	0	13
Eosinophilic lymphogranuloma	0	1	2	0	0	0	3
Inflammation	13	31	9	12	0	0	65
Calcified epithelioma	1	1	0	0	0	0	2
Non-sebaceous lymphoadenoma	0	0	0	1	0	0	1
Lymphoepithelial lesions	0	0	0	3	0	0	3
Nodular fasciitis	0	1	0	0	0	0	1
Myofibromatosis	0	1	0	0	0	0	1
Mucoepidermoid carcinoma	1	6	0	6	6	1	20
Adenocarcinoma , NOS	0	2	0	3	4	0	9
Acinic cell carcinoma	0	13	0	2	0	0	15
Salivary duct carcinoma	0	0	0	1	3	0	4
Adenoid cystic carcinoma	0	4	0	0	3	0	7
Polymorphous adenocarcinoma	0	3	0	5	1	0	9
Uncertainty adenocarcinoma	0	0	1	2	5	0	8
Epithelial-myoepithelial carcinoma	0	1	0	0	0	0	1
Clear cell carcinoma	0	0	0	0	1	0	1
Oncocytic carcinoma	0	0	0	2	0	0	2
Sarcoma	0	1	0	0	0	1	2
Lymphoepithelial carcinoma	0	1	0	2	2	2	7
Malignant lymphoma	0	4	0	3	4	0	11
Malignant melanoma	0	0	0	1	0	0	1
Metastatic solitary fibroma	0	1	0	0	0	0	1
Total	244	637	12	76	30	4	1 003

PI-RADS , Parotid Imaging Reporting and Data System; NOS , nonspecific. The numbers of neoplasms were calculated here.

3 讨论

3.1 影像报告与数据系统的现状

影像报告与数据系统已经在多个器官的影像诊断中广泛应用。1986年美国放射学会(American College of Radiology)最早提出乳腺影像报告与数据系统(Breast Imaging Reporting and Data System, BI-RADS)根据乳腺结节的B超表现,将其分为5个等级,在世界范围内广泛应用,目前已更新至第5版。2009年Horvath等^[8]提出甲状腺影像报告与数据系统(Thyroid Imaging Reporting and Data System, TI-RADS)随后相继出现了妇科影像报告与数据系统、肝脏影像报告与数据系统和前列腺影像报告与数据系统^[9]。2015年,Abdel Razek等^[10]提出的腮腺B超影像报告与数据系统,至今在我国仍未普及应用。

影像学诊断对良恶性肿瘤的判断存在不准确性,肿瘤性疾病的最终诊断大多需依靠组织病理学诊断。基于恶性肿瘤并非一定在影像中表现出恶性征象的临床事实,影像报告与数据系统采用分级诊断的思想对恶性风险概率进行预测,以更好地发挥影像诊断指导临床决策的功能。

3.2 PI-RADS的临床应用价值讨论

传统影像诊断方式对肿瘤性质的判断可以分为确定性诊断和非确定性诊断(可能性诊断和排除性诊断),非确定性诊断所占比例较多,不能有效体现影像诊断对于肿瘤恶性风险的评估。PI-RADS分级诊断方法与传统影像诊断方式相比,有以下优点。(1)有利于临床诊断报告的规范化:传统影像诊断方法用文字描述良性或者恶性肿瘤的确定性和可能性,而PI-RADS则用4个递增等级评价肿瘤的恶性概率,更易于实现规范化的诊断报告,体现影像诊断对肿瘤恶性风险的评估结果。(2)对传统诊断中可以确定良恶性的病例仍具有较好的准确性:BI-RADS与TI-RADS中2级均为确定良性或恶性概率极小的肿瘤,本研究的分级系统中,PI-RADS 2级的恶性肿瘤构成比为0.4%,阴性预测值为99.6%;BI-RADS与TI-RADS中5级为恶性概率较大的肿瘤,TI-RADS 5级的恶性肿瘤概率大于80%,BI-RADS 5级的恶性肿瘤概率大于90%,本研究中PI-RADS 5级的恶性肿瘤概率为96.7%。(3)有利于交界性肿瘤的临床诊断:BI-RADS与TI-RADS中3级和4级用于评价逐渐增加的恶性概率,腺泡细胞癌等恶性肿瘤经常因缺少较特异的影像表现而类似于良性肿瘤,因此,建议将缺少影像特异性表现且无

明显恶性征象的肿瘤(如多形性腺瘤等)诊断为PI-RADS 3级,而将肿瘤表现出一定的恶性征象但仍不充分者诊断为PI-RADS 4级。(4)有利于腮腺炎症性疾病的诊断:根据腮腺疾病的临床特色,本研究建议将一些需与腮腺肿瘤作鉴别诊断的炎症性或免疫性疾病(如干燥综合征结节型、IgG4相关唾液腺炎症性肿块等)诊断为PI-RADS 3b级。(5)有利于增进医患沟通:通过规范诊疗行为,减少了医患纠纷。

本研究虽初步提出了PI-RADS的基本概念,但仍需进行全面深入研究,为其临床应用提供理论基础。首先,需要全面建立基于超声和磁共振成像等常用影像诊断方法的影像报告与数据系统,进一步规范腮腺肿瘤临床影像诊断流程和影像报告方式;目前,基于磁共振的腮腺肿瘤诊断分级系统尚待研究。其次,要进一步全面确定每种影像指标对诊断分级的准确性,进一步筛选影像指标,以利于PI-RADS的推广应用。再次,本研究采用综合分析多种影像指标(如边界、形态、大小、CT值和强化方式等)确定PI-RADS分级的方法,进一步研究需形成确定的诊断思维流程,以利于提高应用PI-RADS诊断的一致性。最后,PI-RADS与传统影像诊断方式相结合,有利于二者取长补短,将会进一步规范临床工作。此外,本研究为回顾性病例研究,纳入的PI-RADS 4级肿瘤病例数量受限,尚需多中心临床研究以进一步验证PI-RADS的临床应用价值。

3.3 PI-RADS与病理类型的相关性

本研究结果提示腮腺肿瘤中良性肿瘤比例为90.2%,良性肿瘤中多形性腺瘤和Warthin瘤合计约占71.6%,与既往研究结果接近^[11]。因此,明确多形性腺瘤和Warthin瘤的影像表现是最为重要的鉴别诊断要点。Warthin瘤的CT表现具有特征性,增强CT诊断Warthin瘤的准确性较高,部分病例可做确定性诊断。本研究中诊断为PI-RADS 2级的病例中约72.1%为Warthin瘤。Warthin瘤中少部分由于囊性变、部位变异或未作增强检查等原因可能会导致诊断准确性降低。多形性腺瘤的影像学表现类型较多,且其影像学表现与组织学类型有密切相关性^[12],上皮细胞为主型、黏液成分丰富型和梗死型多形性腺瘤的影像学表现差别较大^[13]。部分腮腺恶性肿瘤的影像表现接近多形性腺瘤,因此,在影像诊断中如果仅把肿瘤分类为良性和恶性,诊断结果经常导致与病理结果不符,而影像分级诊断方法允许影像医师在4个不同等级的恶性风险中做出评价,更适用于腮腺肿瘤性疾病的影像诊断。

本研究中PI-RADS 2级诊断结果以具有特异性

良性表现或良性可能性较大的肿瘤为主,如脂肪瘤、Warthin 瘤等。PI-RADS 3 级诊断结果包括影像缺少确定性恶性表现的肿瘤,以多形性腺瘤为主。腺泡细胞癌、黏液表皮样癌等一些低度恶性肿瘤在影像中可以表现为边界基本清楚的病变,且缺少确定性的恶性表现,与多形性腺瘤表现难以区分,将此类肿瘤疾病诊断为 PI-RADS 3 级,可以很好地提示临床肿瘤的恶性风险。PI-RADS 4 级肿瘤的恶性风险增加,但仍缺少确定性恶性证据,如明确的较大范围边界不清、周围结构侵犯等,目前,本研究尚缺少足够的证据支持对 PI-RADS 4 级做进一步的划分。本研究结果中 PI-RADS 5 级以腺样囊性癌和黏液表皮样癌为常见,表明随着影像诊断分级增高,恶性肿瘤构成比逐渐增加。

肿瘤边界不清、侵犯毗邻结构、伴有恶性淋巴结、伴有明确的恶性肿瘤临床症状等可以作为影像诊断恶性肿瘤的较为确定的依据。大块不规则钙化影像可能与多形性腺瘤恶变相关;肿瘤的强化特征与具体的病理学类型相关,而不是与良恶性有直接关系。强化特征包括强化的范围性、时期性和强度,常见的唾液腺来源肿瘤中,同等条件下,强化程度由高至低依次是基底细胞腺瘤、Warthin 瘤、黏液表皮样癌、腺样囊性癌、多形性腺瘤,因此,参考强化特征对基底细胞腺瘤和 Warthin 瘤进行预测的准确性较高,但对其他肿瘤的预测准确性欠佳。

腮腺尚有多种肿瘤为交界性肿瘤,如细胞密集型多形性腺瘤^[14]或病理建议需要密切随访的淋巴上皮性病变,其在影像表现上可能也有所差异。因此,建议将缺少影像特异性和确切恶性证据的腮腺肿瘤诊断为 PI-RADS 3~4 级。

3.4 PI-RADS 与临床治疗策略的相关性

PI-RADS 与治疗策略的相关性尚需进一步深入研究。由于可以根据肿瘤的恶性概率做出 PI-RADS 分级诊断,其对指导临床治疗有一定意义。PI-RADS 2 级的腮腺肿瘤治疗可考虑定期随诊观察或择期手术,手术术式可考虑选择保守的腮腺部分切除术等。PI-RADS 3 级和 4 级的腮腺肿瘤由于恶性可能性增加,建议择期手术治疗。PI-RADS 3b 级通常为易与良性肿瘤、恶性肿瘤混淆的炎症性或免疫

性肿块,如干燥综合征结节型、IgG4 相关性唾液腺炎、嗜酸性淋巴肉芽肿等,这些疾病多需要临床进一步相关辅助检查以确诊。PI-RADS 5 级的腮腺肿瘤建议手术治疗,考虑术前活检和术后辅助治疗。

综上所述,应用 PI-RADS 对腮腺肿瘤的临床和影像诊断具有一定的指导意义,有利于提高腮腺肿瘤的临床诊疗水平。

参考文献

- [1] 张震康,俞光岩. 口腔颌面外科学[M]. 2 版. 北京: 北京大学医学出版社,2013.
- [2] Abdullah A, Rivas FF, Srinivasan A. Imaging of the salivary glands [J]. Semin Roentgenol, 2013, 48(1): 65-74.
- [3] 俞光岩,高岩,孙勇刚. 口腔颌面部肿瘤[M]. 北京: 人民卫生出版社,2002.
- [4] Seethala RR, Stenman G. Update from the 4th edition of the World Health Organization classification of head and neck tumours: Tumors of the salivary gland [J]. Head Neck Pathol, 2017, 11(1): 55-67.
- [5] White SC, Pharoah MJ. Oral radiology principles and interpretation [M]. 3rd ed. St. Louis, Missouri: Mosby Elsevier, 2014.
- [6] 马绪臣. 口腔颌面医学影像学[M]. 北京: 北京大学医学出版社,2014.
- [7] 马绪臣,李铁军. 口腔颌面部疾病 CT 诊断与鉴别诊断[M]. 北京: 北京大学医学出版社,2019.
- [8] Horvath E, Majlis S, Rossi R, et al. An ultrasonogram reporting system for thyroid nodules stratifying cancer risk for clinical management [J]. J Clin Endocrinol Metab, 2009, 94(5): 1748-1751.
- [9] Barentsz JO, Richenberg J, Clements R, et al. ESUR prostate MR guidelines 2012 [J]. Eur Radiol, 2012, 22(4): 746-757.
- [10] Abdel Razek AA, Ashmalla GA, Gaballa G, et al. Pilot study of ultrasound parotid imaging reporting and data system (PI-RADS): Inter-observer agreement [J]. Eur J Radiol, 2015, 84(12): 2533-2538.
- [11] 马大权,俞光岩. 唾液腺病学[M]. 2 版. 北京: 人民卫生出版社,2014.
- [12] Kim H, Kim SY, Kim YJ, et al. Correlation between computed tomography imaging and histopathology in pleomorphic adenoma of parotid gland [J]. Auris Nasus Larynx, 2018, 45(4): 783-790.
- [13] Ito FA, Jorge J, Vargas PA, et al. Histopathological findings of pleomorphic adenomas of the salivary glands [J]. Med Oral Patol Oral Cir Bucal, 2009, 14(2): E57-61.
- [14] 黄敏娴,马大权,俞光岩,等. 复发性涎腺多形性腺瘤的临床与病理分析[J]. 现代口腔医学杂志,2008, 22(1): 1-4.
(2019-10-10 收稿)
(本文编辑:赵波)